Hindawi
Journal of Sensors
Volume 2018, Article ID 8096064, 8 pages
https://doi.org/10.1155/2018/8096064

Research Article

Multilayer Distributed Circuit Modeling for Galvanic Coupling Intrabody Communication

Zhi Ying Chen,[1,2,3] **Yue Ming Gao**,[3,4] **and Min Du**[4,5]

[1]*College of Electrical Engineering & Automation, Fuzhou University, Fuzhou, Fujian 350116, China*
[2]*School of Electrical Engineering & Automation, Xiamen University of Technology, Xiamen, Fujian 361024, China*
[3]*Key Laboratory of Medical Instrumentation & Pharmaceutical Technology of Fujian Province, Fuzhou University, Fuzhou, Fujian 350116, China*
[4]*College of Physics and Telecommunication Engineering, Fuzhou University, Fuzhou, Fujian 350116, China*
[5]*Fujian Provincial Key Laboratory of Eco-Industrial Green Technology, Wuyi University, Wuyishan, Fujian 354300, China*

Correspondence should be addressed to Yue Ming Gao; fzugym@163.com and Min Du; dm_dj90@163.com

Received 28 August 2017; Revised 19 November 2017; Accepted 11 December 2017; Published 11 March 2018

Academic Editor: Alberto J. Palma

Characterization of the human body as a transmission medium for electrical signals is a necessity for using intrabody communication (IBC) technique into connecting wearable electronic sensors and devices. In this paper, we propose a novel multilayer distributed circuit model for galvanic-coupling type IBC, which is emphasized on the propagation characteristics in contrast with other IBC models. Based on the model, a program is written in MATLAB to investigate the propagation characteristics of a human body channel with the frequency of 10 MHz to 20 MHz and the distance of 5 cm to 10 cm. Finally, a galvanic coupling IBC measurement is implemented to verify the proposed model. The outcome proves that the model is valid and correct.

1. Introduction

Intrabody communication (IBC) is a promising wireless communication technology which was first mentioned by Zimmerman in 1995 [1]. It is a technique that uses the human body as a transmission channel for electrical signals. Compared with other wireless communication technologies, it helps to meet the high requirements of low power consumption, miniaturized volume, and security for electronic devices wore on the body or implanted in the body [2]. There are two basic methods of signal coupling between the transmitter and the receiver in an IBC system: capacitive coupling and galvanic coupling [3]. In the capacitive coupling approach, only two signal electrodes are attached to the skin, and both transmitter (TX) and receiver (RX) ground electrodes remain floating, which is easily affected by noisy environment because the signal return path is closed through the surrounding environment and external ground [4]. In the galvanic coupling approach, which is focused on this paper, an electrical signal is applied differentially and then received by means of a pair of TX electrodes and a pair of RX electrodes attached to the skin. In this way, the human body between TX and RX can be considered as a transmission line (waveguide) in where the signal propagates. In order to understand the galvanic coupling IBC behavior better, it is significant to investigate the propagation mechanism of a human body channel. There are many different methods having been proposed for galvanic coupling IBC modeling [5–10], such as finite element method (FEM) model, quasi-static field theory model, equivalent electrical circuit model, and distributed circuit model. In [5], a realistic 3-D finite element method model of the human arm has been presented with a frequency range of 1 kHz to 100 MHz and a distance range of 5 cm to 20 cm. In [6], a quasi-static field model of the human limb at the frequency of 1 kHz to 1 MHz has been solved analytically and the gain for a single channel length of 6 cm has been obtained. In [7], a simplified equivalent circuit model of the human arm has been proposed for IBC with of

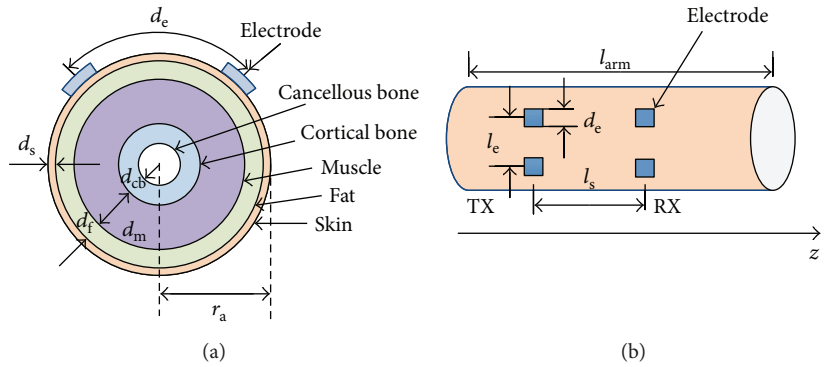

Figure 1: Geometry of the proposed model. (a) Transverse section of the arm composed of five concentric layers of tissues: skin, fat, muscle, cortical bone, and cancellous bone. (b) Longitudinal view of the arm with electrodes, depicting parameters such as channel length (l_s), interelectrode distance (l_e), and arm length (l_{arm}).

frequency range 200 kHz to 10 MHz and channel length 7.5 cm to 11 cm. A similar simplified circuit model has also been put forward in [8] with frequency range from 1 kHz to 1 MHz and channel length from 5 cm to 30 cm. A multipath circuit model through layered tissues has been given in [9], where the study frequency is from 100 kHz to 1 MHz and the channel length is from 5 cm to 40 cm. In [10], a distributed circuit model focusing on the propagation characteristics has been investigated for both IBC coupling techniques, where the frequency and channel length are, respectively, considered from 10 kHz to 1 MHz and from 5 cm to 15 cm for galvanic coupling IBC. However, most of the models listed above mainly study the case of low-frequency (generally below 1 MHz) galvanic coupling IBC. Furthermore, a majority of the models are not simple and accurate enough to explain the experimental results of galvanic coupling IBC. FEM models [5, 6] need a quite complicated and large calculation. Additionally, they are usually built based on quasi-static field theory in which the wavelength is required to be much larger than the dimensions of the studied body domain. According to [4, 11, 12], beyond 10 MHz and particularly at larger TX-to-RX distances, the body's antenna effect increases, so the simulation frequency up to 100 MHz in [5] is not appropriate and the correctness of the obtained result remains a doubt. In the simplified equivalent circuit modeling [7–9], the impedance of the human body is calculated based on lump parameter rather than distributed parameter, and this kind of equivalence is not proper for high-frequency IBC because of the wave effect at frequencies higher than about 10 MHz [12–14]. The distributed circuit model [10] only takes the distributed parameter effect of the skin layer into account and ignores the distributed parameters of the fat and muscle tissues. As we know, the wave propagation effects cannot be negligible definitely as the frequency increases, and the communication no longer follows a formal IBC scheme. Thus, further research is still needed in order to develop more accurate models to identify the propagation mechanisms of IBC performance.

Consequently, with the objective of high-speed short-range communication in wireless body area network (WBAN), in this paper, we propose a novel multilayer distributed circuit model to investigate the propagation mechanisms of galvanic coupling-type IBC. For the human forearm, we write a program in MATLAB to calculate the voltage gains of a body channel based on the proposed model with the frequency of 10 MHz to 20 MHz and propagation distance of 5 cm to 10 cm. At the same time, we have also carried out some experimental measurements using harmonized galvanic coupling setups to validate the proposed model. It should be noted that the frequency range in our study is much higher than any other existing galvanic coupling IBC research. Therefore, this model will be quite valuable for the galvanic coupling IBC in high-speed communication which is the limitation of the current galvanic coupling IBC.

This paper is organized as follows: Section 2 presents a multilayer distributed circuit model for galvanic coupling IBC. Section 3 describes the calculation results of the proposed model. Section 4 presents the galvanic coupling IBC measurement setup and its comparative results with the proposed model. Finally, Section 5 presents the conclusions of this paper.

Table 1: Geometry parameters of the human forearm.

Parameter	Value	Description
r_a (cm)	5	Arm radius
l_{arm} (cm)	60	Arm length
d_s (mm)	1.5	Skin thickness
d_f (mm)	8.5	Fat thickness
d_m (mm)	27.5	Muscle thickness
d_{cb} (mm)	6	Cortical bone thickness
d_e (mm)	4	Electrode side length
l_e (cm)	8	Interelectrode distance
l_s (cm)	5, 6.5, 8, 10	Signal channel length

2. The Proposed Model

2.1. Geometry Model Definition for the Human Forearm. In this paper, the human forearm is simplified as a multilayer cylinder formed by five different concentric layers, each of which simulates a different tissue: skin, fat, muscle, cortical bone, and cancellous bone. The detailed geometry is shown in Figure 1, and the parameters are listed in Table 1. The

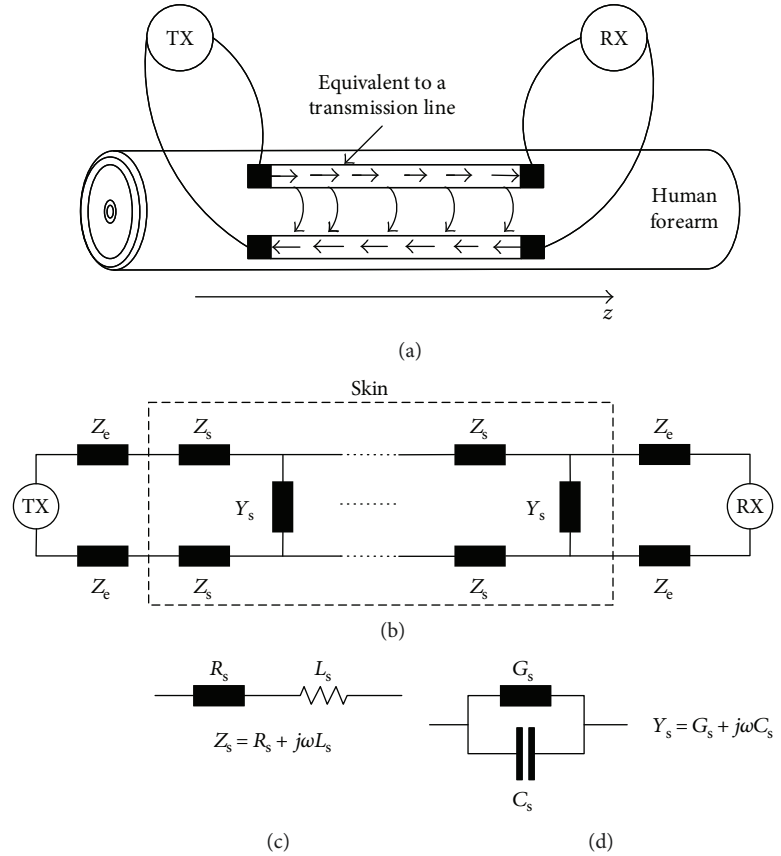

Figure 2: Equivalent distributed circuit of the skin layer. (a) Galvanic coupling-type IBC. (b) Distributed circuit of the skin layer. (c) Impedance of the skin (Z_s). (d) Conductance of the skin (Y_s).

tissue thicknesses are within the range of true anatomical proportions and refer to those proposed in [5]. Two pairs of squared TX and RX electrodes are placed on the skin at the determined distance l_e and l_s. The AC signal is applied on TX and is transmitted to RX along the z-axis.

2.2. Multilayer Distributed Circuit Modeling for the Human Forearm. The human forearm can be seen as a lossy multilayer transmission line consisted of multilayer distributed circuits, because the signal from TX to RX propagates in a multipath channel composed of the different tissue layers of skin, fat, muscle, and bones. Each of the human tissue layer is equivalent to a distributed circuit consisted of the periodic insertion of basic cells formed by the impedance $Z(\omega)$ and the admittance $Y(\omega)$, defined on the same plane, with the objective of studying their influence on propagation characteristics. The impedance $Z(\omega)$ is composed of the resistance $R(\omega)$ and the inductance $L(\omega)$, where $R(\omega)$ and $L(\omega)$, respectively, emulate the resistive characteristic and inductive effect of the human tissues in the signal propagation between the basic cells repeated along the propagation axis. The admittance $Y(\omega)$ is represented as a shunt circuit composed of a conductance $G(\omega)$ and a susceptance $B(\omega)$, where $G(\omega)$ emulates the conductive pathways of the tissue and $B(\omega)$ accounts for the electric field effect. Both $G(\omega)$ and $B(\omega)$ are defined on the longitudinal direction between two points placed on the same plane. For instance, the equivalent distributed parameter circuit of the skin layer is shown in Figure 2, where Z_e is the equivalent impedance of the electrode and Z_s and Y_s are the distributed impedance and admittance of skin, respectively. We can see that the distributed parameter elements Z_s and Y_s shown in the dotted box are repeated with the longitudinal direction to represent the propagation characteristics of the signal in the skin tissue. The other tissue layers, such as fat and muscle, are modeled as well, and the final detail model scheme is shown in Figure 3. It should be noticed that the model is consisted of only three layers of distributed circuits: skin, fat, and muscle. The bone layer is not considered because the corresponding circuit of human forearm geometry model is symmetrical and the conductivity of bones is much lower than other tissues, which causes almost no current to flow in the bone tissue. In addition, the circuits between layers are connected by the equivalent distributed admittances that emulate the conduction of the signal from skin to fat and fat to muscle in the radial direction. In Figure 3, Z_s and Y_s, Z_f and Y_f, and Z_m and Y_m are, respectively, the per-unit-distance impedances and admittances of the skin, fat, and muscle. Y_{sf} and Y_{fm} are, respectively, the per-unit-distance admittances of skin to fat and fat to muscle.

2.3. Impedance and Admittance of Human Tissues. The frequency behavior of dielectric properties of tissues, such as

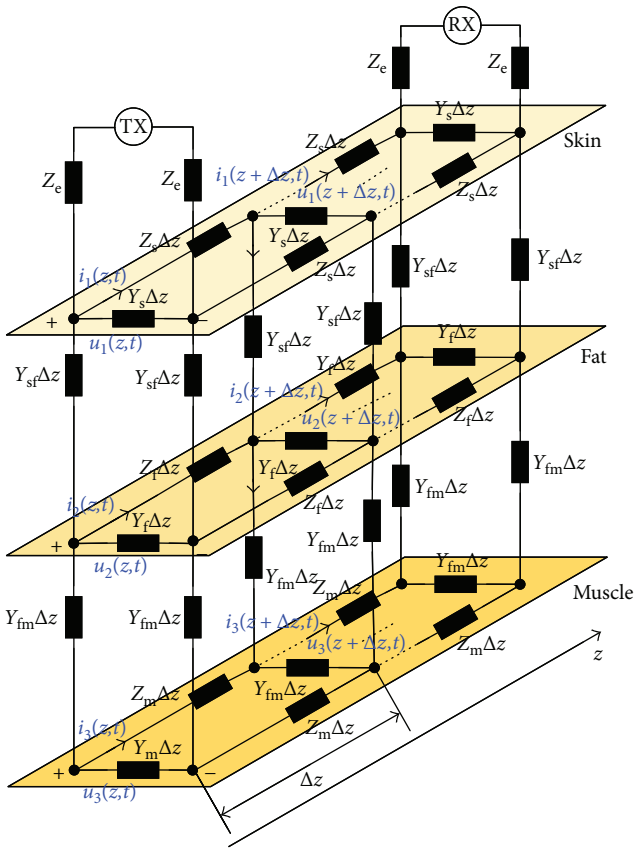

Figure 3: Multilayer distributed circuit model of galvanic coupling IBC for the human forearm.

conductivity and permittivity, is derived from the parametric modes of Gabriel et al. [15] who summarized measurements from *in vivo* experiments on the human body and autopsies of cadavers and animals. The four-order Cole–Cole equation [15] presents the change of dielectric properties of a tissue over a broad frequency range 10 Hz–100 GHz:

$$\varepsilon_r^*(\omega) = \varepsilon_\infty + \sum_{n=1}^{4} \frac{\Delta\varepsilon_n}{1 + (j\omega\tau_n)^{(1-\alpha_n)}} + \frac{\sigma_i}{j\omega\varepsilon_0}, \tag{1}$$

where ε_r^* is the complex dielectric constant, $\Delta\varepsilon_n$ is the magnitude of the dispersion which is calculated from the difference between permittivity at static ε_s and infinite frequency ε_∞, ω is the angular frequency, τ_n is the relaxation time constant which depends on physical processes such as ion effects, α_n is the distribution parameter which is between 0 and 1, σ_i is the static ionic conductivity, and ε_0 is the permittivity of vacuum.

Once ε_r^* is obtained from (1), it can be divided into real and imaginary parts [16] as follows:

$$\varepsilon_r^*(\omega) = \varepsilon'(\omega) - j\varepsilon''(\omega). \tag{2}$$

Then, the relative permittivity $\varepsilon_r(\omega)$ and conductivity $\sigma(\omega)$ can be given as follows:

$$\begin{aligned} \varepsilon_r(\omega) &= \varepsilon'(\omega), \\ \sigma(\omega) &= \omega\varepsilon_0\varepsilon''(\omega). \end{aligned} \tag{3}$$

Next, the conductance and capacitance of each tissue are easily written as follows:

$$\begin{aligned} G(\omega) &= \sigma(\omega)K, \\ C(\omega) &= \varepsilon_0\varepsilon_r(\omega)K, \\ K &= \frac{S}{l}, \end{aligned} \tag{4}$$

where K is the ratio of the cross-sectional area to the length of tissues, S is the cross-sectional area, and l is the length which is generally set as 1 m in distributed parameter calculation.

Finally, the per-unit-distance impedances of basic cell on each tissue layer with propagation direction are easily calculated from

$$Z(\omega) = R(\omega) = \frac{1}{G(\omega)}, \tag{5}$$

and the per-unit-distance admittances of basic cell on each tissue layer between two points on the same plane are obtained by the following:

$$Y(\omega) = G(\omega) + j\omega C(\omega). \tag{6}$$

It should be noted that the inductive element L is neglected in this circuit configuration.

2.4. Equations of the Model. We assume that the signal propagates along the z-axis. Our model consists of a line section of the length Δz containing impedances $Z_s\Delta z$, $Z_f\Delta z$, and $Z_m\Delta z$ and admittances $Y_s\Delta z$, $Y_f\Delta z$, $Y_m\Delta z$, $Y_{sf}\Delta z$, and $Y_{fm}\Delta z$ in Figure 3.

Our objective is to determine the manner and extent to which the output voltage and current are changed from their input values in the limit as the length Δz approaches a very small value. We can consequently obtain a group of differential equations that describe the variations of the voltage and current with respect to z. First, the input and output voltages and currents of each layer circuit are given, respectively, as $u_n(z,t)$ and $i_n(z,t)$ and $u_n(z+\Delta z,t)$ and $i_n(z+\Delta z,t)$, with $n = 1, 2, 3$. Then, Kirchhoff's voltage law (KVL) and Kirchhoff's current law (KCL) are applied to the circuit encompassing the entire section length, and we obtain the following:

$$
\begin{aligned}
u_1(z,t) &= 2Z_s\Delta z i_1(z,t) + u_1(z+\Delta z,t),\\
u_2(z,t) &= 2Z_f\Delta z i_2(z,t) + u_2(z+\Delta z,t),\\
u_3(z,t) &= 2Z_m\Delta z i_3(z,t) + u_3(z+\Delta z,t),\\
i_1(z,t) &= i_1(z+\Delta z,t) + Y_s\Delta z u_1(z+\Delta z,t)\\
&\quad + Y_{sf}\Delta z\frac{u_1(z+\Delta z,t)-u_2(z+\Delta z,t)}{2},\\
i_2(z,t) &= i_2(z+\Delta z,t) + Y_f\Delta z u_2(z+\Delta z,t)\\
&\quad + Y_{fm}\Delta z\frac{u_2(z+\Delta z,t)-u_3(z+\Delta z,t)}{2}\\
&\quad - Y_{sf}\Delta z\frac{u_1(z+\Delta z,t)-u_2(z+\Delta z,t)}{2},\\
i_3(z,t) &= i_3(z+\Delta z,t) + Y_m\Delta z u_3(z+\Delta z,t)\\
&\quad - Y_{fm}\Delta z\frac{u_2(z+\Delta z,t)-u_3(z+\Delta z,t)}{2}.
\end{aligned}
\tag{7}
$$

Now, in the limit, as Δz approaches zero (or a value small enough to be ignored), we obtain the final differential equation form to describe the multilayer distributed circuit model as follows:

$$
\begin{aligned}
\frac{\partial}{\partial z}u &= \mathbf{A}i,\\
\frac{\partial}{\partial z}i &= \mathbf{B}u,
\end{aligned}
\tag{8}
$$

where

$$
u = \begin{bmatrix} u_1\\ u_2\\ u_3 \end{bmatrix},
$$

$$
i = \begin{bmatrix} i_1\\ i_2\\ i_3 \end{bmatrix},
$$

$$
\mathbf{A} = \begin{bmatrix} -2Z_s & 0 & 0\\ 0 & -2Z_f & 0\\ 0 & 0 & -2Z_m \end{bmatrix},
$$

$$
\mathbf{B} = \begin{bmatrix} -Y_s - \frac{1}{2}Y_{sf} & \frac{1}{2}Y_{sf} & 0\\ \frac{1}{2}Y_{sf} & -\frac{1}{2}Y_{sf} - Y_f - \frac{1}{2}Y_{fm} & \frac{1}{2}Y_{fm}\\ 0 & \frac{1}{2}Y_{fm} & -Y_m - \frac{1}{2}Y_{fm} \end{bmatrix},
\tag{9}
$$

where $\mathbf{A}$ and $\mathbf{B}$ are, respectively, called the net series impedance matrix and the net shunt admittance matrix in the multilayer transmission line—both as per-unit-distance measures.

2.5. Solutions of the Model Equations. Once the equations of multilayer distributed circuit are obtained, the final solution of voltage and current distribution with respect to z can be derived by using the Laplace transform and inverse Laplace transform.

With the help of Laplace transformation, (8) is transformed as follows:

$$
\begin{aligned}
s(U(s) - u(0)) &= \mathbf{A}I(s),\\
s(I(s) - i(0)) &= \mathbf{B}U(s),
\end{aligned}
\tag{10}
$$

where $u(0)$ and $i(0)$ are the initial values of voltage and current corresponding to $z = 0$; they are also the initial values corresponding to $t = 0$.

When the source voltage is imposed on TX at the moment of $t = 0$, the current has not flowed into the body yet, so we give the values of $u(0)$ and $i(0)$ as follows:

$$
\begin{aligned}
u(0) &= \begin{bmatrix} V_i\\ 0\\ 0 \end{bmatrix},\\
i(0) &= \begin{bmatrix} 0\\ 0\\ 0 \end{bmatrix},
\end{aligned}
\tag{11}
$$

where V_i is the sinusoidal voltage source applied on the two TX electrodes.

Substituting $u(0)$ and $i(0)$ into (12), we therefore can obtain the following:

$$
\begin{aligned}
U(s) &= \left(s^2 - \mathbf{AB}\right)^{-1} su(0),\\
I(s) &= B\left(s^2 - \mathbf{AB}\right)^{-1} u(0).
\end{aligned}
\tag{12}
$$

Finally, the inverse Laplace transforms of $U(s)$ and $I(s)$ are given by the following:

$$
\begin{aligned}
u(z) &= L^{-1}(U(s)),\\
i(z) &= L^{-1}(I(s)).
\end{aligned}
\tag{13}
$$

These are the solutions of the multilayer distributed circuit model. With these solutions, the received voltage and current by RX electrodes at any distance z can be figured out, and the voltage gain of the body channel is achieved by the following:

$$
\text{gain} = 20\log_{10}\left(\frac{V_o}{V_i}\right),
\tag{14}
$$

where V_o is the received voltage.

3. Results of the Model

The proposed model is carried out by writing a program in MATLAB to study the gain of the received voltage with the

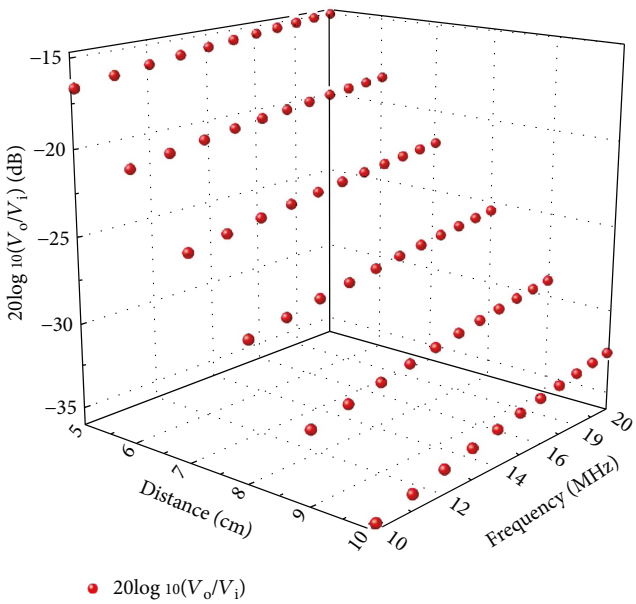

FIGURE 4: Gain of the received voltage corresponding to the distance z and frequency.

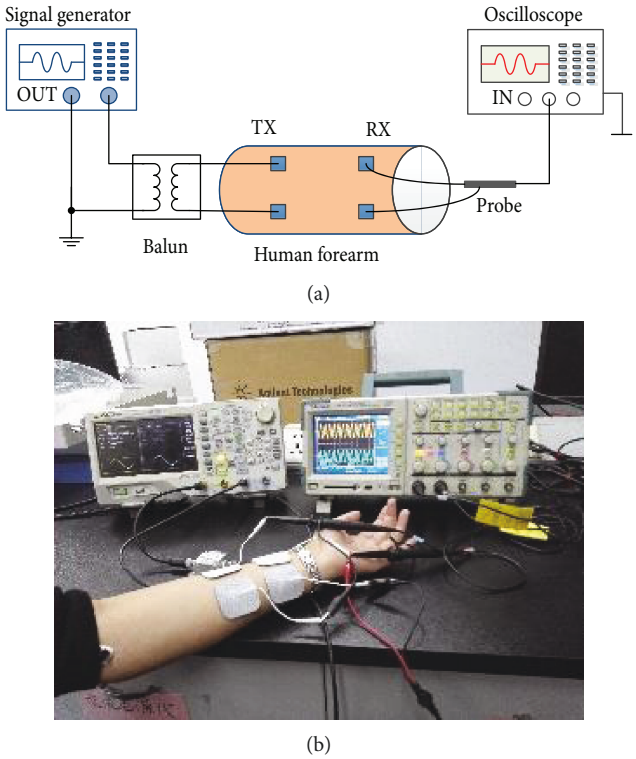

FIGURE 5: Galvanic coupling measurement setup. (a) Measurement circuit. (b) Measurement scene.

distance z from 5 cm to 10 cm and the frequency from 10 MHz to 20 MHz. The results are shown in Figure 4. We can see the gain increases with the rise in frequency, which indicates that the property of body channel performs as a high band-pass characteristic with respect to the frequency of 10 MHz to 20 MHz. We also see that the gain presents a linear decrease with distance z, which reveals that the received voltage decays exponentially with the signal propagation direction z.

4. Galvanic Coupling Measurement Setup

In order to validate the results of the proposed model, a galvanic coupling IBC measurement on a human forearm is carried out. The setup is consisted of a signal generator DG4162 and a balun FTB-1-6 at the transmitter side (TX), a digital isolation oscilloscope TPS2024 at the receiver side (RX), and four 4 cm × 4 cm medical electrodes LT-1 attached to the skin in a differential configuration in Figure 5 [17]. It should be noticed that a differential probe must be used to test the received signal voltage so that the electromagnetic interference from the AC source can be eliminated. The excited signal between the two transmitter electrodes adopts a sine voltage with the peak-to-peak value of 3 V and the frequency of the range from 10 MHz to 20 MHz. In addition, with the purpose of analyzing the effect of channel length to the transmission quality, different channel lengths l_s, 5 cm, 6.5 cm, and 8 cm, are tested.

Figure 6 shows the comparison of gain between the multilayer distributed circuit model and the experiment on a 37-year-old female volunteer for the galvanic coupling IBC. In Figure 6, the measurement values are averaged from the results of a three-day repeated experiment. It can be found that the result approaches to that of the measurement, where the difference values between them are all less than 4 dB. Table 2 lists, in detail, the specific values of the proposed model and measurement when $z = 5$ cm. The maximum and the minimum difference values are 3 dB and 0.03 dB, respectively. However, from Figure 6, we also find that the measured results started lower than the simulated results at the low-frequency end (10 MHz) and then crossed over and ended up higher than the simulated results at the high-frequency end (20 MHz). This may be caused by the parasitic capacitances between the electrodes, which generally perform high pass characteristics and is worth validating in a later study. In the actual propagation, as the frequency increases, the air nearby the body channel may be the other path of signal transmission and is presented in the form of parasitic capacitances. Whereas in our proposed model, we suppose the body channel as a waveguide line where the signal mainly propagates. In this case, the deviation between the two results is reasonable. So, the proposed model is correct and valid. It also proves that multilayer distributed circuit model is suitable for investigating the propagation characteristics of galvanic coupling IBC.

5. Conclusion

In this paper, a novel multilayer distributed circuit model for galvanic coupling IBC on a human forearm has been proposed to investigate the propagation characteristics of a body channel. Based on the model, we find that a human body channel presents as a high band-pass characteristic with the frequency from 10 MHz to 20 MHz, and the signal is

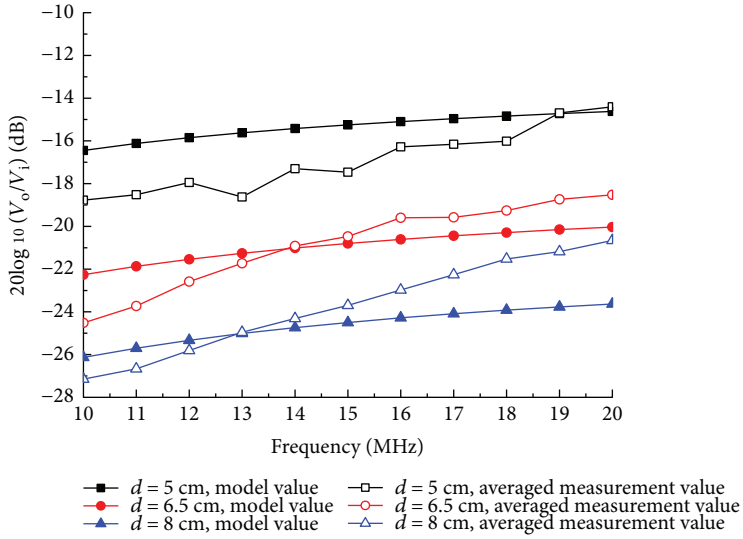

Figure 6: Comparison of the results between the IBC measurement and model.

Table 2: Comparison of the gain values between the IBC measurement and model corresponding to the distance $z = 5$ cm.

Frequency (MHz)	Value of model (dB)	Averaged value of measurement (dB)	Difference (dB)
10	−16.45	−18.77	2.32
11	−16.12	−18.52	2.40
12	−15.85	−17.94	2.09
13	−15.62	−18.62	3.00
14	−15.42	−17.30	1.88
15	−15.25	−17.46	2.21
16	−15.1	−16.28	1.18
17	−14.96	−16.16	1.20
18	−14.84	−16.01	1.17
19	−14.72	−14.69	0.03
20	−14.62	−14.41	0.21

exponentially attenuating with the increasing of propagation distance along the body. It illustrates that the human forearm is like a multilayer lossy transmission line which has some similar characteristics with respect to the general transmission line. To validate the accuracy of the model, an IBC experiment on a human forearm has been carried out, and the results demonstrate that the proposed model based on multilayer distributed circuit meets the actual situation of high-frequency galvanic coupling IBC which other models do not focus. Though the model is fulfilled at the frequency of 10 MHz to 20 MHz, it may be applied to a higher frequency, for example, 400 MHz, and the experimental probe will be done in our next important work. Considering that a body channel may be affected by the sizes and types of different electrodes, we will take a deep study on the electrodes and account it into modeling in the next step. Moreover, we will also focus on extending the model to other parts of the human body and the possible application of these findings to the design of wireless medical healthcare devices in the future.

Conflicts of Interest

The authors declare that there is no conflict of interest regarding the publication of this paper.

Acknowledgments

This work was supported by the National Natural Science Foundation of China under Grant no. U1505251, the Chinese Ministry of Science and Technology, Project no. 2016YFE0122700, and the New Century Excellent Talents Program of the Department of Education, Fujian Province, China.

References

[1] T. G. Zimmerman, *Personal Area Networks: Near-Field Intra-Body Communication [M.S. Thesis]*, MIT Media Lab., Cambridge, MA, USA, 1995.

[2] T. Kobayashi, Y. Shimatani, and M. Kyoso, "Application of near-field intra-body communication and spread spectrum technique to vital-sign monitor," in *2013 7th International Symposium on Medical Information and Communication Technology (ISMICT)*, pp. 4517–4520, Tokyo, Japan, March 2013.

[3] M. Seyedi, B. Kibret, D. T. H. Lai, and M. Faulkner, "A survey on intrabody communications for body area network applications," *IEEE Transactions on Biomedical Engineering*, vol. 60, no. 8, pp. 2067–2079, 2013.

[4] Z. Lucev, I. Krois, and M. Cifrek, "A capacitive intrabody communication channel from 100 kHz to 100 MHz," *IEEE Transactions on Instrumentation and Measurement*, vol. 61, no. 12, pp. 3280–3289, 2012.

[5] M. Amparo Callejon, J. Reina-Tosina, D. Naranjo-Hernandez, and L. M. Roa, "Galvanic coupling transmission in Intrabody communication: a finite element approach," *IEEE*

Transactions on Biomedical Engineering, vol. 61, no. 3, pp. 775–783, 2014.

[6] S. H. Pun, Y. M. Gao, P. U. Mak, M. I. Vai, and M. Du, "Quasi-static modeling of human limb for intra-body communications with experiments," *IEEE Transactions on Information Technology in Biomedicine*, vol. 15, no. 6, pp. 870–876, 2011.

[7] B. Kibret, M. Seyedi, D. T. Lai, and M. Faulkner, "Investigation of galvanic-coupled intrabody communication using the human body circuit model," *IEEE Journal of Biomedical and Health Informatics*, vol. 18, no. 4, pp. 1196–1206, 2014.

[8] K. Hachisuka, Y. Terauchi, Y. Kishi et al., "Simplified circuit modeling and fabrication of intrabody communication devices," in *The 13th International Conference on Solid-State Sensors, Actuators and Microsystems, 2005. Digest of Technical Papers. TRANSDUCERS '05*, vol. 1, pp. 461–464, Seoul, South Korea, South Korea, June 2005.

[9] M. Swaminathan, F. S. Cabrera, J. S. Pujol, U. Muncuk, G. Schirner, and K. R. Chowdhury, "Multi-path model and sensitivity analysis for galvanic coupled intra-body communication through layered tissue," *IEEE Transactions on Biomedical Circuits and Systems*, vol. 10, no. 2, pp. 339–351, 2016.

[10] M. A. Callejón, D. Naranjo-Hernandez, J. Reina-Tosina, and L. M. Roa, "Distributed circuit modeling of galvanic and capacitive coupling for Intrabody communication," *IEEE Transactions on Biomedical Engineering*, vol. 59, no. 11, pp. 3263–3269, 2012.

[11] J. Bae, H. Cho, K. Song, H. Lee, and H. J. Yoo, "The signal transmission mechanism on the surface of human body for body channel communication," *IEEE Transactions on Microwave Theory and Techniques*, vol. 60, no. 3, pp. 582–593, 2012.

[12] N. Cho, J. Yoo, S.-J. Song, J. Lee, S. Jeon, and H. J. Yoo, "The human body characteristics as a signal transmission medium for intrabody communication," *IEEE Transactions on Microwave Theory and Techniques*, vol. 55, no. 5, pp. 1080–1086, 2007.

[13] W. Jianqing, Y. Nishikawa, and T. Shibata, "Analysis of on-body transmission mechanism and characteristic based on an electromagnetic field approach," *IEEE Transactions on Microwave Theory and Techniques*, vol. 57, no. 10, pp. 2464–2470, 2009.

[14] K. Fujii, M. Takahashi, and K. Ito, "Electric field distributions of wearable devices using the human body as a transmission channel," *IEEE Transactions on Antennas and Propagation*, vol. 55, no. 7, pp. 2080–2087, 2007.

[15] S. Gabriel, R. W. Lau, and C. Gabriel, "The dielectric properties of biological tissues: III. Parametric models for the dielectric spectrum of tissues," *Physics in Medicine and Biology*, vol. 41, no. 11, pp. 2271–2293, 1996.

[16] Z. Chen, Y. Gao, and M. Du, "Electromagnetic wave transmission characteristics on different tissue boundaries for implantable human body communication," *Chinese Journal of Radio Science*, vol. 32, no. 2, pp. 134–143, 2017.

[17] Z. Chen, Y. Gao, and M. Du, "A study of galvanic-coupled intra-Body communication based on circuit-coupled finite element model," in *2015 IEEE International Conference on Consumer Electronics*, China, Shenzhen, April, 2015.